Optical Materials 36 (2014) 760–763

Contents lists available at ScienceDirect

Optical Materials

journal homepage: www.elsevier.com/locate/optmat

Generation of 1.3 μm and 1.5 μm high-energy Raman radiations in α-$BaTeMo_2O_9$ crystals

Shande Liu, Junjie Zhang, Zeliang Gao, Lei Wei, Shaojun Zhang, Jingliang He *, Xutang Tao *

State Key Laboratory of Crystal Materials, Shandong University, Jinan 250100, China

ARTICLE INFO

Article history:
Received 2 September 2013
Received in revised form 4 November 2013
Accepted 17 November 2013
Available online 12 December 2013

Keywords:
α-$BaTeMo_2O_9$ crystals
1.5 μm Raman laser
Comparison of Raman gain coefficient

ABSTRACT

The generations of high energy 2nd- and 3rd-order stimulated Raman scattering lasers based on the α-$BaTeMo_2O_9$ crystal were demonstrated for the first time. The Raman gain coefficient has been compared with that of the YVO_4 crystal. A maximum total Stokes radiation energy of 27.3 mJ was obtained, containing 20.1 mJ 2nd-order Stokes energy at 1318 nm, together with 7.2 mJ 3rd-order Stokes energy at 1497 nm, giving an overall conversion efficiency of 35.9% and a slope efficiency of 54.5%. With an optical coating design, a total 3rd- and 4th-order Stokes energy of 16.5 mJ was generated. The maximum energy for 4th-order Stokes radiation at 1731 nm was 2 mJ. The pulse durations for the 2nd-, 3rd-, and 4th-order Stokes shift were 10 ns, 8.6 ns, and 5.2 ns, respectively. Our experimental results show that the α-BTM crystal is a promising Raman crystal for the generations of eye-safe radiations.

1. Introduction

Besides the optical parametric processes (such as SHG, SFG, OPO), the stimulated Raman scattering (SRS) is another well-known technique widely used for generating the new frequency coherent radiations [1–3]. In recent years, solid-state Raman crystals such as nitrate, tungstate, carbonate, and molybdate crystals [4–8] have attracted a lot due to their intrinsically high concentration of Raman-active centers as well as the favorable thermal and mechanical properties [9]. With the improvement of crystal quality, a number of high-energy solid-state Raman lasers have been developed rapidly, which can generate the radiations in the eye-safe spectral utilized in the fields of medicine, free-space communication, laser ranging and etc. [10–12].

Very recently, a novel Raman crystal, named orthorhombic $BaTeMo_2O_9$ (α-BTM), has been synthesized and grown with high quality by our group [13], which physical and chemical properties were described in details in Ref. [14]. Maczka analyzed the vibrational modes of the α-BTM crystal based on the classical lattice dynamics calculations [15], and the most intense Raman shift was related to the stretching vibration of Mo–O bonds. Experimentally, the first-order Stokes shift with a maximum pulse energy of 15.1 mJ was obtained, under a pulsed 1064 nm laser pumped [16]. Moreover, the 2nd- and 3rd-order Stokes shifts of the α-BTM crystal are located at eye-safe spectral band for the potential applications in medicine, communication, and laser ranging, thus studies on high order Stokes shift are greatly expected.

In this paper, a high-energy 2nd- and 3rd-order SRS laser sources pumped by a pulsed 1064 nm Nd:YAG laser was realized based on the α-BTM crystal for the first time. A maximum output energy of 27.3 mJ was obtained, with 20.1 mJ 2nd-order Stokes energy at 1318 nm and 7.2 mJ 3rd-order Stokes energy at 1497 nm, corresponding to an overall conversion efficiency of 35.9% and a slope efficiency of 54.5%. With an optical coating design, a total 3rd- and 4th-order Stokes energy of 16.5 mJ was generated, giving an optical-to-optical efficiency of 21.7% and a slope efficiency of 32.6%. The 3rd-order Stokes energy at 1497 nm and 4th-order Stokes energy at 1731 nm were 14.5 mJ and 2 mJ, respectively.

2. Comparisons of Raman gain coefficient between α-BTM and YVO_4 crystals

According to the rate equation model describing the Raman laser, the Raman gain is an important factor that determines the Stokes threshold and conversion efficiency. As is well known, the Raman gain is determined by the Raman gain coefficient and the length of the Raman crystals. The Raman gain coefficient related to the Raman crystal can be expressed by [17]:

$$g_{ss} = \frac{8\pi Nc^2}{\hbar n_s^2 \omega_s^3 \Delta\gamma_R}\left(\frac{d\sigma}{d\Omega}\right) \quad (1)$$

where N is the number density of molecules, n_s and ω_s are the refractive index and radian frequency at the Stokes wavelength, $d\sigma/d\Omega$ is the Raman scattering cross section, and $\Delta\gamma_R$ is the

* Corresponding authors. Tel.: +86 531 88366129; fax: +86 531 88366119 (J. He). Tel.: +86 531 88364963; fax: +86 531 88574135 (X. Tao).
E-mail addresses: jlhe@sdu.edu.cn (J. He), txt@sdu.edu.cn (X. Tao).

0925-3467/$ - see front matter © 2013 Elsevier B.V. All rights reserved.
http://dx.doi.org/10.1016/j.optmat.2013.11.021

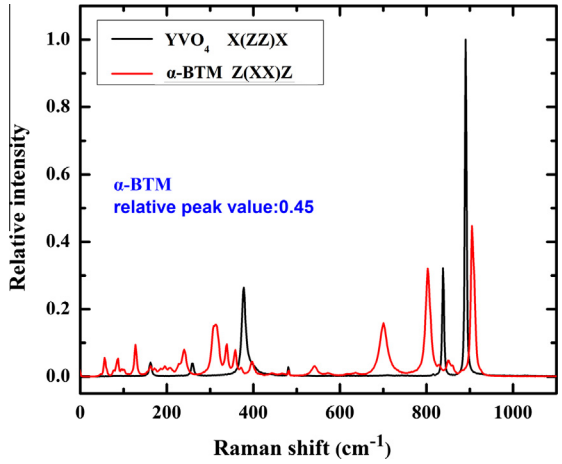

Fig. 1. Relative spontaneous Raman scattering spectra of YVO_4 and α-BTM crystals.

linewidth of the Raman transition. The value of $(d\sigma/d\Omega)(\Delta\gamma_R)^{-1}$ can be characterized as the peak intensity in the measured spontaneous Raman scattering spectrum. Therefore, the relative Raman gain coefficient of two different crystals can be calculated by comparing the spontaneous Raman scattering spectra. In addition, the correction factor M, representing the effects of the difference in refractive index should be considered and is given by [18,19]:

$$M = \frac{n_{s1}^2}{n_{s2}^2} \cdot \frac{(1-R_{S2}^P)(1-R_{S2}^S)}{(1-R_{S1}^P)(1-R_{S1}^S)} \tag{2}$$

where n and R are the refractive index and the reflectivity of Raman crystal, respectively. Superscripts P and S denote the pump and Stokes wavelengths. In this paper, YVO_4 and α-BTM crystals were chosen for comparative study. The spontaneous Raman scattering spectrum of these two crystals was measured using a Raman spectrometer (Horiba JY HR800), and the excitation wavelength was 532 nm. As shown in Fig. 1 the peak intensity ratio was 0.45 between the YVO_4 and α-BTM crystals under identical experimental conditions. Therefore, the relative Raman gain coefficient of α-BTM can be written as:

$$g_{rel}(\alpha\text{-BTM}) = \frac{N_{\text{BTM}} \cdot n_{s,\text{YVO4}}^2 \cdot 0.45 \cdot M}{N_{\text{YVO4}} \cdot n_{s,\text{BTM}}^2} \tag{3}$$

with $N_{\text{BTM}} = 5.36$, $n_{s,\text{BTM}} = 2.034$ [14], $N_{YVO_4} = 4.22$, $n_{s,YVO_4} = 2.239$, and $M = 0.77$, The parameter g_{rel} was calculated to be about 0.53.

3. Experimental setup

The configuration of the α-BTM Raman laser is shown in Fig. 2. The pump source was a lamp-pumped electro-optic Q-switched Nd:YAG laser amplifier system operating in TEM_{00} mode at 1064 nm with a pulse width of 14 ns and a repetition rate of 1 Hz. The spot diameter on the α-BTM crystal surface was measured to be about 2 mm, and the divergence angle of the beam was less than 3 mrad. An α-BTM Raman-active crystal with a size of $5 \times 5 \times 39\ \text{mm}^3$ was cut along the Z-direction with both sides polished but uncoated. The cavity mirrors M_1, M_2, and M_3 were all the plane mirrors and the optical coating parameters were shown in Table 1. The output pulse energy was measured using an energy meter, and the pulse characteristics were recorded using a digital oscilloscope (Tektronix, DPO7104) and a photodetector (New Focus, 1611). An optical spectrum analyzer (AvaSpec-3648-NIR-256-2.2) was used to measure the Stokes spectrum.

Table 1
The optical coating parameters for the mirrors M_1, M_2, and M_3.

Wavelength (nm)	M_1	M_2		M_3	
		T_{oc1}	T_{oc2}	T_{oc3}	T_{oc4}
1064 (pump)	100%	0	0	0	0
1177 (1st-order)	0	0	0	0	0
1318 (2nd-order)	0	58%	36%	0	0
1497 (3rd-order)	0	62%	61%	35%	20%

4. Results and discussions

Firstly, the dual-wavelength operation Raman laser was studied with the α-BTM crystal. The Raman cavity was consisted of two flat mirrors M_1 and M_2. The total output pulse energy at the 2nd- and 3rd-order Stokes wavelengths for different output couplers versus the pump pulse energy are shown in Fig. 3. It can be seen that there is slight difference for the thresholds between the output coupler T_{oc1} and T_{oc2}, which can be attributed to the high reflectivity coating of the mirrors at the 1st-order Stokes wavelength. The threshold for the 2nd-order Stokes was primarily determined by the length of the Raman crystal and the threshold for the 1st-order Stokes generation. Once the 1st-order Stokes generation was initiated, the 2nd-order Stokes oscillation was excited. This observation demonstrated that the high-order Stokes emissions are initialized not at a spontaneous level of Raman scattering, but amplified in an intense filed stimulated by the pump and the 1st-order Stokes radiations [20]. A maximum total output pulse energy of 27.3 mJ was obtained under the pump pulse energy of 76 mJ with an

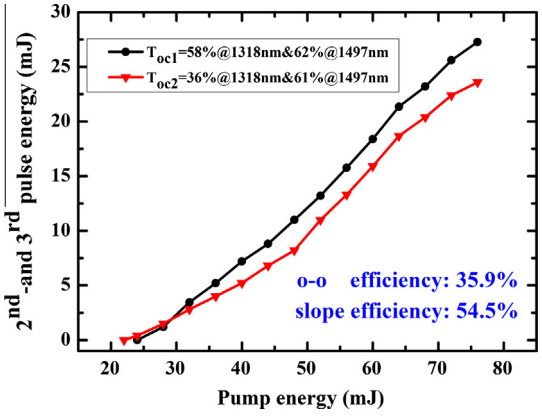

Fig. 3. The 2nd- and 3rd-order total output pulse energy versus the pump pulse energy.

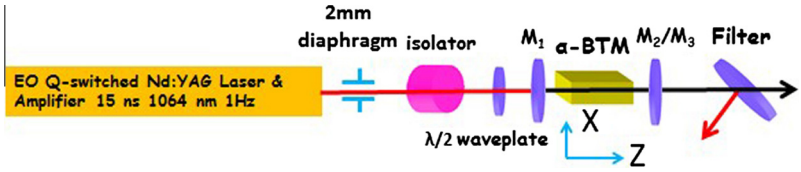

Fig. 2. Set up for eye-safe α-BTM Raman lasers.

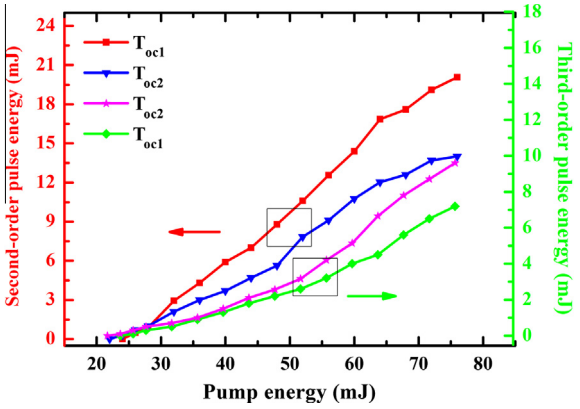

Fig. 4. Individual output pulse energy at 2nd- and 3rd-order wavelengths with respect to the pump pulse energy.

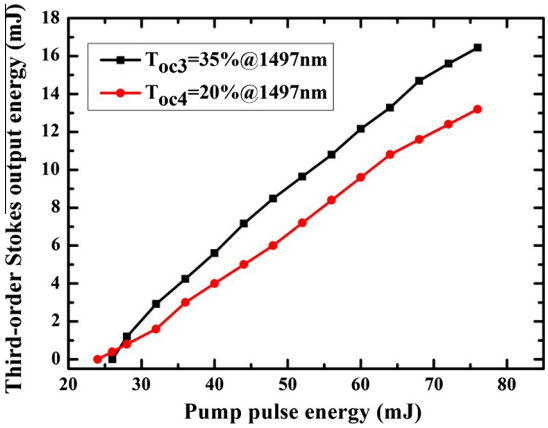

Fig. 5. Relationships between the 3rd- and 4th-order Stokes output pulse energy and the pump pulse energy.

output coupling T_{oc1}, corresponding to an optical-to-optical conversion efficiency of 35.9% and a slope efficiency of 54.5%. With the output coupler T_{oc2}, a total maximum output pulse energy of 23.6 mJ was achieved, under the same pump energy. By using a filter, the 2nd- and 3rd-order Stokes output energy were separated from each other. The separated output energies versus the pump pulse energy are shown in Fig. 4. The maximum 2nd- and 3rd-order Stokes pulse energy of 20.1 mJ and 7.2 mJ were obtained with the output coupler T_{oc1}. With the output coupler T_{oc2}, the 2nd- and 3rd-order Stokes pulse energy were 14 mJ and 9.6 mJ, respectively. Although the 2nd-order Stokes output pulse energy with the output coupler T_{oc1} was larger than that of output coupler T_{oc2}, the maximum 3rd-order Stokes pulse energy was generated by employing the output coupler T_{oc2}. As we know, SRS is a cascading nonlinear frequency conversion process, that is, the generation of high-order Stokes radiation requires low-order Stokes radiation as the pump source. Therefore, there is a balance point for the simultaneous dual-wavelength operation Raman laser between the high and low-order Stokes output. Output coupler T_{oc1} with high transmission for the 2nd-order Stokes radiation would output more energy from the cavity than that of the output coupler T_{oc2}, thus limited the conversion from the 2nd- to 3rd-order Stokes due to the relatively low intracavity intensity on the contrary.

In order to obtain a high energy Stokes radiation output at 1.5 μm, the output coupler M_2 was replaced by an output coupler M_3. The laser cavity was formed by the mirrors M_1 and M_3, with both the 1st- and 2nd-order Stokes wavelengths oscillating simultaneously. The relationship between the 3rd- and 4th-order Stokes output pulse energy and the pump pulse energy is shown in Fig. 5. A maximum total Stokes output pulse energy of 16.5 mJ was obtained with the output coupler T_{oc3}, including a 3rd-order Stokes pulse energy of 14.5 mJ and a 4th-order Stokes pulse energy of 2 mJ, giving an optical-to-optical efficiency of 21.7% and a slope efficiency of 32.6%.

The 2nd-, 3rd-, and 4th-order Stokes output wavelengths were located at 1318 nm, 1497 nm, and 1731 nm, respectively, and the output spectra are shown in Fig. 6. Fig. 6a was obtained by using the output coupler M_2, and Fig. 6b was obtained using the output coupler M_3, which corresponded well to the stretching vibration of Mo–O bonds.

The pulse durations of the Stokes shifts were measured under the maximum pump energy as shown in Fig. 7. The 10 ns pulse duration of the 2nd-order Stokes radiation obtained in our experiments was a little smaller than that of the pump pulse. The 3rd- and 4th-order Stokes pulse width was 8.6 ns and 5.2 ns, respectively.

5. Conclusions

In conclusion, we have demonstrated the high-energy Raman lasers at 1.3 μm and 1.5 μm based on a α-$BaTeMo_2O_9$ crystal pumped by a pulsed 1064 nm Nd:YAG laser. The Raman gain coefficient has been compared to that of YVO_4 crystal and the ratio was

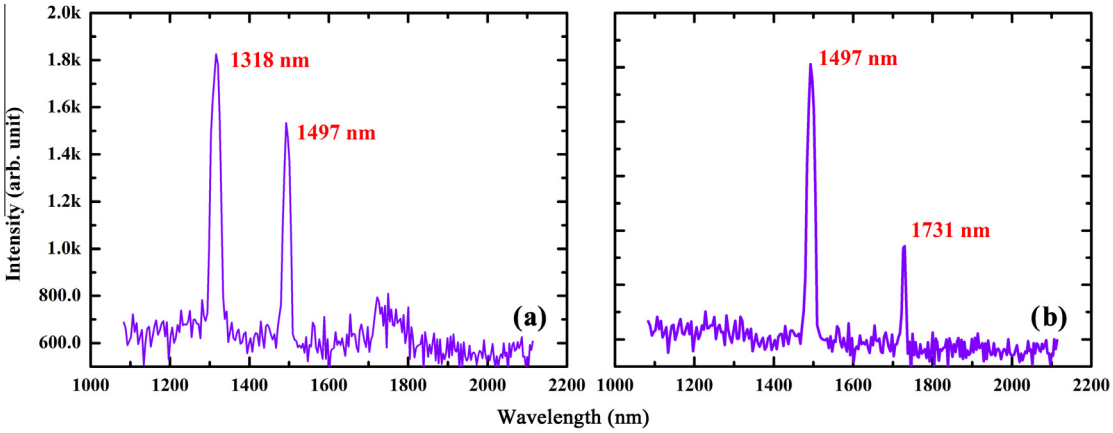

Fig. 6. The Stokes output spectra for 2nd-, 3rd-, and 4th-order wavelengths.

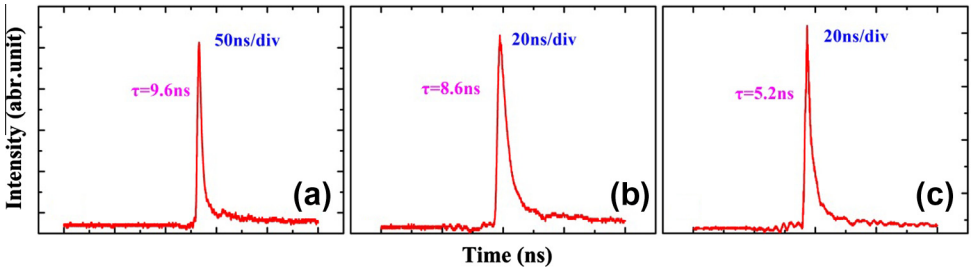

Fig. 7. Pulse profile for Stokes laser pulse (a) 2nd-order (b) 3rd-order and (c) 4th-order.

about 0.53. A 20.1 mJ 2nd-order Stokes radiation at 1318 nm and a 7.2 mJ 3rd-order Stokes radiation at 1497 nm were obtained under a maximum pump pulse energy of 76 mJ, giving an overall conversion efficiency of 35.9% and a slope efficiency of 54.5%. By using a cavity resonating at the 2nd-order Stokes wavelength, a maximum total pulse energy of 16.5 mJ for the high-order Stokes was generated, corresponding to an optical-to-optical efficiency of 21.7% and a slope efficiency of 32.6%. The maximum 4th-order Stokes pulse energy at 1731 nm was 2 mJ. The pulse durations for the 2nd-, 3rd-, and 4th-order Stokes radiations were 10 ns, 8.6 ns, and 5.2 ns, respectively. The high-energy Raman radiations are expected to be applied in many fields such as medicine, communication, laser ranging and ecology.

Acknowledgements

This work was supported by the National Natural Science Foundation of China (Grant Nos. 51021062, 51272129, 51227002, 91022003, 61308088), the 973 Program of the People's Republic of China (Grant No. 2010CB630702), and the Program of Introducing Talents of Disciplines to Universities in China (111 Program No. b06017). S.D. Liu would like to thank the graduate independent innovation foundation of Shandong University (Grant No. yzc12115).

References

[1] P.G. Zverev, T.T. Basiev, A.M. Prokhorov, Opt. Mater. 11 (1999) 335.
[2] J.T. Murray, R.C. Powell, N. Peyghambarian, D. Smith, W. Austin, R.A. Stolzenberger, Opt. Lett. 20 (1995) 1017.
[3] J.Q. Zhao, X.L. Zhang, X. Guo, X.J. Bao, L. Li, J.H. Cui, Opt. Lett. 38 (2013) 1206.
[4] V.A. Lisinetskii, A.S. Grabtchikov, I.A. Khodasevich, H.J. Eichler, V.A. Orlovich, Opt. Commun. 272 (2007) 509.
[5] V.A. Lisinetskii, H.J. Eichler, H. Rhee, X. Wang, V.A. Orlovich, Opt. Commun. 281 (2008) 2227.
[6] A.A. Kaminskii, Laser Photon. Rev. 1 (2007) 93.
[7] L.I. Ivleva, T.T. Basiev, I.S. Voronina, P.G. Zverev, V.V. Osiko, N.M. Polozkov, Opt. Mater. 23 (2003) 439.
[8] A.A. Kaminskii, L. Bohatý, H. Rhee, A. Kaltenbach, O. Lux, H.J. Eichler, R. Rückamp, P. Becker, Laser Photon. Rev. 7 (2013) 425.
[9] N. Takei, S. Suzuki, F. Kannari, Appl. Phys. B 74 (2002) 521.
[10] J.J. Zhang, Z.L. Gao, S.D. Liu, S.J. Zhang, W.G. Zhang, X.X. Feng, P. Zhao, J.L. He, X.T. Tao, Appl. Phys. Exp. 6 (2013) 072702.
[11] Y.X. Fan, Y. Liu, Y.H. Duan, Q. Wang, L. Fan, H.T. Wang, G.H. Jia, C.T. Tu, Appl. Phys. B 93 (2008) 327.
[12] Y.F. Chen, Opt. Lett. 29 (2004) 2172.
[13] J.J. Zhang, Z.H. Zhang, W.G. Zhang, Q.X. Zheng, Y.X. Sun, C.Q. Zhang, X.T. Tao, Chem. Mater. 23 (2011) 3752.
[14] J.J. Zhang, Z.H. Zhang, Y.X. Sun, C.Q. Zhang, X.T. Tao, Cryst. Eng. Commun. 13 (2011) 6985.
[15] M. Maczka, W. Paraguassu, P.T.C. Freire, A. Majchrowski, P.S. Pizani, J. Phys.: Condens. Matter 25 (2013) 125404.
[16] S.D. Liu, J.J. Zhang, Z.L. Gao, S.J. Zhang, J.L. He, X.T. Tao, Appl. Phys. Exp. 6 (2013) 042401.
[17] J.A. Piper, H.M. Pask, IEEE J. Sel. Top. Quantum 13 (2007) 692.
[18] F.L. Galeener, J.C. Mikkelsen Jr., R.H. Geils, W.J. Mosby, Appl. Phys. Lett. 32 (1978) 34.
[19] H.T. Huang, D.Y. Shen, J.L. He, Opt. Exp. 20 (2012) 27838.
[20] P.G. Zverev, T.T. Basiev, I.V. Ermakov, A.M. Prokhorov, Proc. SPIE 2498 (1994) 164.